CHAPTER 4

RESULTS AND DISCUSSION

4.1 Binding of single platinum atom on SWCNTs

The closed-end caps for (3,3), (4,4) and (5,5) armchair SWCNTs can be representative of closed-end caps for various lengths of closed-end SWCNTs, as no effect of SWCNTs length has been assumed. C-C bonds for these optimized structures were labeled as binding positions of Pt clusters for geometrical construction of Pt-decorated SWCNTs. The B3LYP/GEN-optimized geometries of Pt-decorated on closed-end (3,3), (4,4) and (5,5) armchair SWCNT of which C-C bonds are defined as shown in Figure 3.1. All structures of a single platinum atom adsorbed on (3,3), (4,4) and (5,5)SWCNTs are shown in Figures 4.1, 4.2 and 4.3., respectively. Their binding energies and relative energies are shown in Table 4.1.

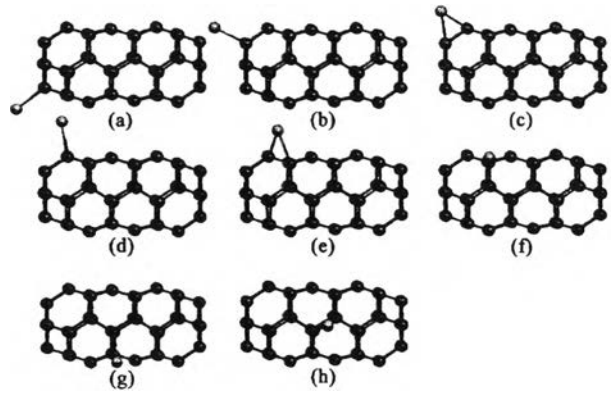

Figure 4.1 The B3LYP/GEN-optimized structures of Pt-decorated on closed-end (3,3) armchair SWCNT of which C-C bonds are defined as types (a) 1, (b) 2, (c) 3, (d) 4, (e) 5, (f) 6, (g) 7 and (h) 8.

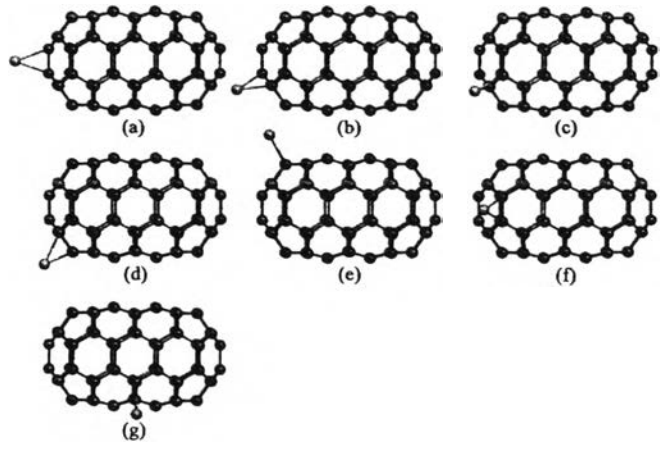

Figure 4.2 The B3LYP/GEN-optimized structures of Pt-decorated on closed-end (4,4) armchair SWCNT of which C-C bonds are defined as types (a) 1, (b) 2, (c) 3, (d) 4, (e) 5, (f) 6 and (g) 7.

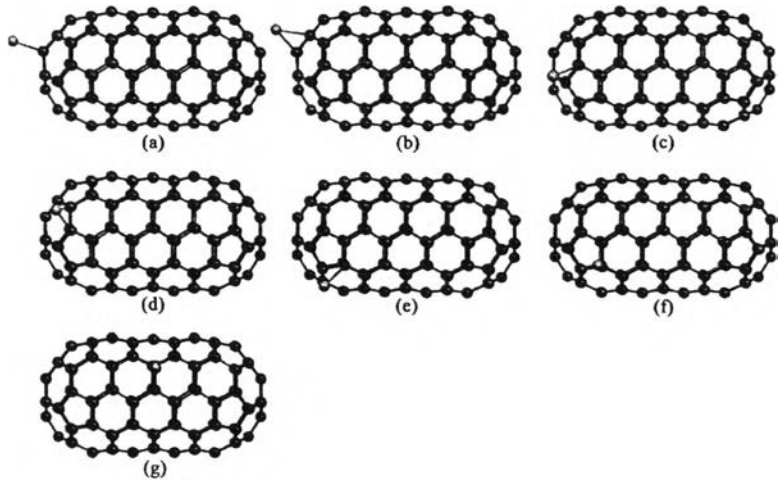

Figure 4.3 The B3LYP/GEN-optimized structures of Pt-decorated on closed-end (5,5) armchair SWCNT of which C-C bonds are defined as types (a) 1, (b) 2, (c) 3, (d) 4, (e) 5, (f) 6 and (g) 7.

Table 4. 1 Binding energies of platinum atom adsorbed on sidewall of various sizes of closed-end SWCNTs and relative energies of their binding structures.

Single Pt atom on SWCNTs	$\Delta E_{binding}$ [a]	ΔE_{rel} [a]
Single Pt adatom on (3,3)SWCNTs		
Pt(1)/(3,3)SWCNT	-52.38	0.00
Pt(2)/(3,3)SWCNT	-31.00	21.37
Pt(3)/(3,3)SWCNT	-33.78	18.60
Pt(4)/(3,3)SWCNT	-35.71	16.66
Pt(5)/(3,3)SWCNT	-43.78	8.59
Pt(6)/(3,3)SWCNT	-26.09	26.28
Pt(7)/(3,3)SWCNT	-26.69	25.68
Pt(8)/(3,3)SWCNT	-23.11	29.27
Single Pt adatom on (4,4)SWCNTs		
Pt(1)/(4,4)SWCNT	-22.00	10.14
Pt(2)/(4,4)SWCNT	-24.70	7.44
Pt(3)/(4,4)SWCNT	-28.93	3.21
Pt(4)/(4,4)SWCNT	-14.83	17.31
Pt(5)/(4,4)SWCNT	-32.14	0.00
Pt(6)/(4,4)SWCNT	-15.61	16.53
Pt(7)/(4,4)SWCNT	-7.56	24.58
Single Pt adatom on (5,5)SWCNTs		
Pt(1)/(5,5)SWCNT	-6.92	12.73
Pt(2)/(5,5)SWCNT	-18.05	1.60
Pt(3)/(5,5)SWCNT	-8.34	11.30
Pt(4)/(5,5)SWCNT	-19.65	0.00
Pt(5)/(5,5)SWCNT	-3.64	16.06
Pt(6)/(5,5)SWCNT	-6.66	12.99
Pt(7)/(5,5)SWCNT	-4.67	14.98

[a] In kcal/mol.

As they are all conformers of Pt/(3,3)SWCNT type, the most stable conformer is Pt(1)/(3,3)SWCNT and the second most is Pt(5)/(3,3)SWCNT of which binding energies are -52.38 and -43.78 kcal/mol, respectively. The most and second most

stable conformers for a single platinum atom adsorbed on the (4,4)SWCNT are Pt(5)/(4,4)SWCNT and Pt(3)/(4,4)SWCNT of which binding energies are −32.14 and -28.93 kcal/mol, respectively. For the most and second most stable conformers for a single platinum atom adsorbed on the (5,5)SWCNT are Pt(4)/(5,5)SWCNT and Pt(2)/(5,5)SWCNT of which binding energies are −19.65 and −18.05 kcal/mol, respectively. The binding abilities of single platinum atom to SWCNTs based on the most favorable configurations are in order: (3,3)SWCNT > (4,4)SWCNT > (5,5)SWCNT. As diameters (d, in nm) for (3,3), (4,4) and (5,5)SWCNTs computed using formula, $d = 0.078(n^2 + m^2 + nm)^{\frac{1}{2}}$ [38], relation between their diameters against their binding energies is shown in Figure 4.4. The equation of a polynomial fit,

$\Delta E_{\text{binding}} = -159.6 + 350.60d - 212d^2$ was obtained.

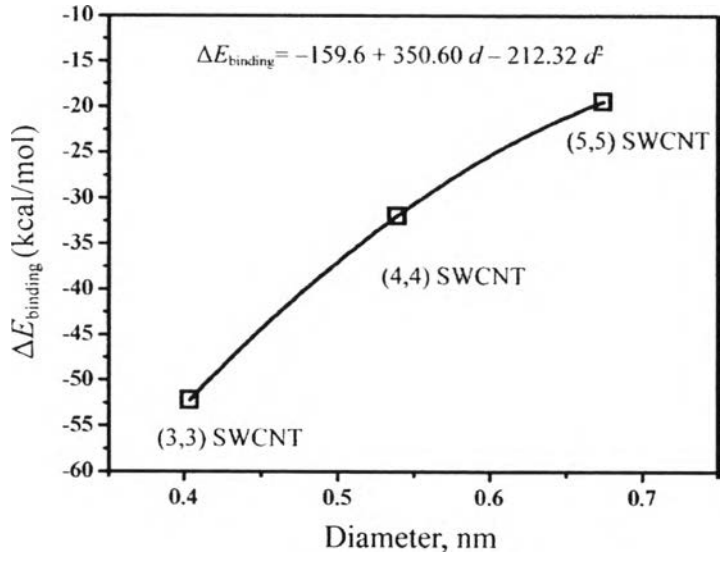

Figure 4.4 Plot between binding energies of single platinum atom on (3,3), (4,4) and (5,5) armchair SWCNTs against their diameters (d). Polynomial fitted equation is shown on top.

The preferred structures of a single platinum atom adsorbed on (3,3), (4,4) and (5,5)SWCNTs are quite similar conformations of which a single platinum atom is likely adsorbed on C-C bond at closed-end cap area.

Energy gaps, chemical indices and dipole moment of clean SWCNTs and their structures decorated by single atom and clusters of platinum are shown in Table A1, in Appendix. Dipole moments of all clean SWCNTs are found to be zero and the Pt_4/(5,5)SWCNT has the highest dipole moment (4.50 Debye). It shows that energy gaps of adsorption configurations of platinum single atom on SWCNTs are slightly different as compared with clean SWCNTs of their corresponding except clean (3,3)SWCNT. This probably means that platinum atom and clusters on the (4,4) and (5,5)SWCNTs slightly affect reactivities of the (4,4) and (5,5)SWCNTs.

4.2 Hydrogen adsorption on single platinum atom decorated SWCNTs

Adsorption energies of H_2 to Pt atom decorated on closed-end (3,3), (4,4) and (5,5)SWCNTs are shown in Table 4.2. It shows that the strongest adsorptions for hydrogen gas adsorbed on single platinum atom of Pt/SWCNTs occur on the Pt(4)/(3,3)SWCNT (ΔE_{ads}=-33.26 kcal/mol), Pt(2)/(4,4)SWCNT (ΔE_{ads}=-33.47 kcal/mol) and Pt(5)/(5,5)SWCNT (ΔE_{ads}=-23.53 kcal/mol). All adsorption structures of hydrogen molecule adsorbed on single platinum atom of Pt/(3,3), Pt/(4,4) and Pt/(5,5)SWCNTs are shown in Figure 4.5, 4.6 and 4.7, respectively. All the hydrogen adsorptions on single platinum atom of Pt-decorated SWCNTs are chemisorption.

Table 4.2 Adsorption energies of H_2 to Pt atom(s) decorated on closed-end SWCNTs.

Hydrogen adsorption	ΔE_{ads} [a]
On Pt atom/(3,3)SWCNTs:	
H_2/Pt(1)/(3,3)SWCNT	-18.63
H_2/Pt(2)/(3,3)SWCNT	-24.54
H_2/Pt(3)/(3,3)SWCNT	-23.31
H_2/Pt(4)/(3,3)SWCNT	-33.26
H_2/Pt(5)/(3,3)SWCNT	-28.37
H_2/Pt(6)/(3,3)SWCNT	-8.14
H_2/Pt(7)/(3,3)SWCNT	-25.82
H_2/Pt(8)/(3,3)SWCNT	-25.89
On Pt atom/(4,4)SWCNTs:	
H_2/Pt(1)/(4,4)SWCNT	-13.85
H_2/Pt(2)/(4,4)SWCNT	-33.47
H_2/Pt(3)/(4,4)SWCNT	-22.49
H_2/Pt(4)/(4,4)SWCNT	-25.33
H_2/Pt(5)/(4,4)SWCNT	-32.01
H_2/Pt(6)/(4,4)SWCNT	-16.20
H_2/Pt(7)/(4,4)SWCNT	-28.77
On Pt atom/(5,5)SWCNTs:	
H_2/Pt(1)/(5,5)SWCNT	-22.41
H_2/Pt(2)/(5,5)SWCNT	-20.10
H_2/Pt(3)/(5,5)SWCNT	-22.45
H_2/Pt(4)/(5,5)SWCNT	-20.23
H_2/Pt(5)/(5,5)SWCNT	-23.53
H_2/Pt(6)/(5,5)SWCNT	-20.77
H_2/Pt(7)/(5,5)SWCNT	-21.80

[a] In kcal/mol.

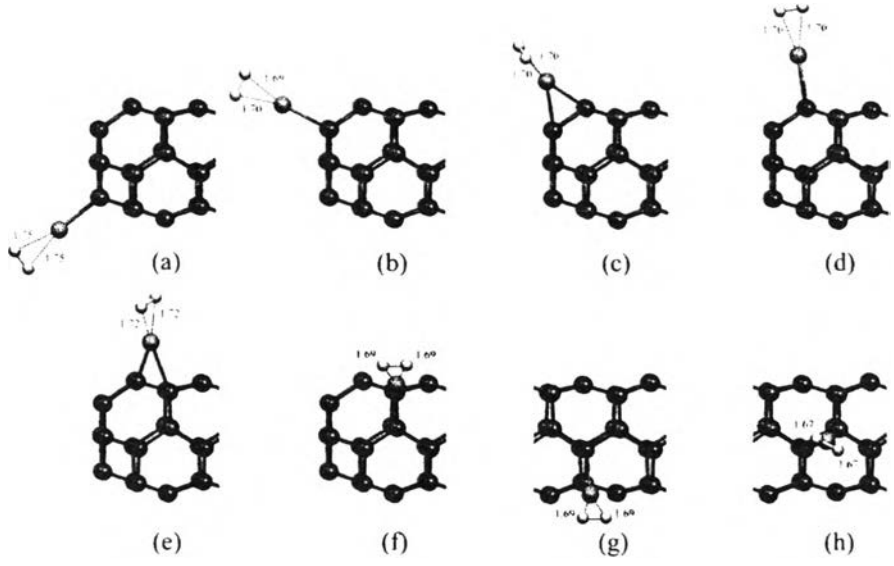

Figure 4.5 The B3LYP/GEN-optimized structures of adsorption configurations of H_2 on Pt atom in the Pt-decorated closed-end (3,3) armchair SWCNTs on C-C types (a) 1, (b) 2, (c) 3, (d) 4, (e) 5, (f) 6, (g) 7 and (h) 8. Their bond distances are in Å.

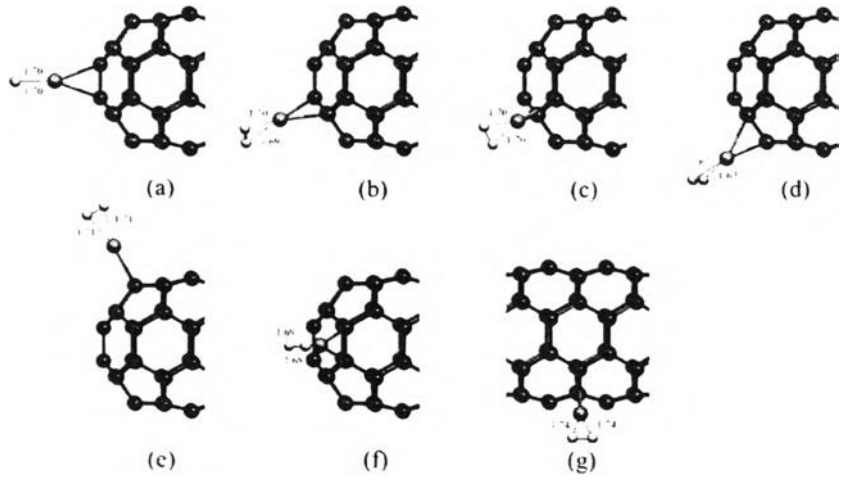

Figure 4.6 The B3LYP/GEN-optimized structures of adsorption configurations of H_2 on Pt atom in the Pt-decorated closed-end (4,4) armchair SWCNTs on C-C types (a) 1, (b) 2, (c) 3, (d) 4, (e) 5, (f) 6 and (g) 7. Their bond distances are in Å.

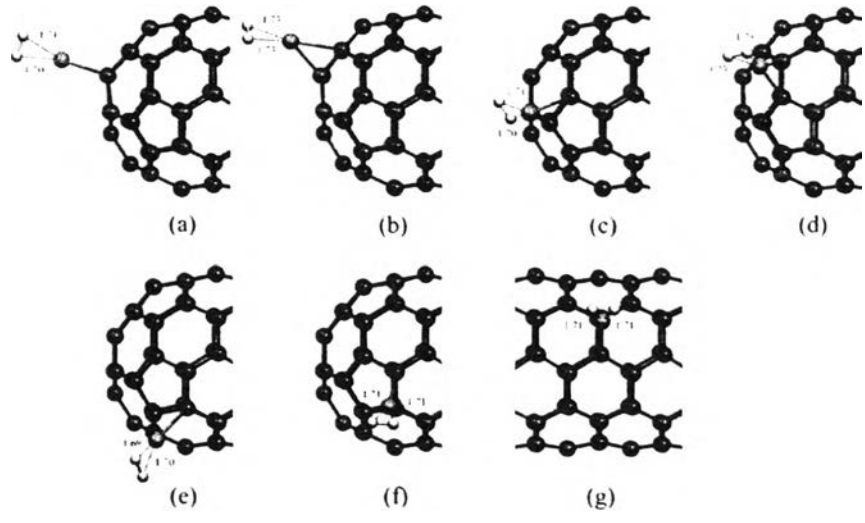

Figure 4.7 The B3LYP/GEN-optimized structures of adsorption configurations of H_2 on Pt atom in the Pt-decorated closed-end (5,5) armchair SWCNTs on C-C types (a) 1, (b) 2, (c) 3, (d) 4, (e) 5, (f) 6 and (g) 7. Their bond distances are in Å.

4.3 Binding of platinum cluster (n=2 to 4) on SWCNTs

The most stable structures of platinum clusters decorated on C-C bonds at closed-end cap were obtained and the configurations are shown in Figures 4.8, 4.9 and 4.10 for Pt_n/(3,3), Pt_n/(4,4) and Pt_n/(5,5)SWCNTs, respectively.

Binding energies for platinum clusters (Pt_n, n=2 to 4) adsorbed on sidewall of various sizes of closed-end SWCNTs are shown in Table 4.3. The binding abilities on (3,3), (4,4) and (5,5)SWCNTs are in same order: $Pt_4 > Pt_3 > Pt_2$. The binding abilities of platinum clusters on the (3,3)SWCNT are slightly different but on the (5,5)SWCNT are much different. For the same size of platinum clusters, binding abilities are in order: (3,3)SWCNT > (4,4)SWCNT > (5,5)SWCNT. Nevertheless, binding abilities of Pt_4 on (3,3), (4,4) and (5,5)SWCNTs are high.

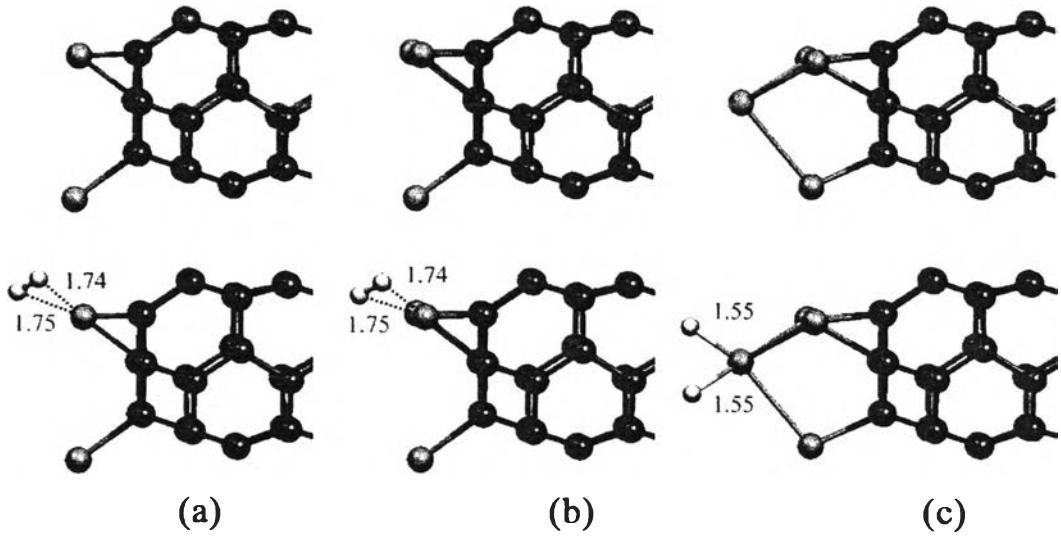

Figure 4.8 The B3LYP/GEN-optimized structures of adsorption configurations of H_2 adsorbed on Pt atom of the Pt cluster-decorated (3,3)SWCNTs whose Pt cluster are (a) Pt_2, (b) Pt_3 and (c) Pt_4. Top images are their bare Pt_n/SWCNTs structures. Their bond distances are in Å.

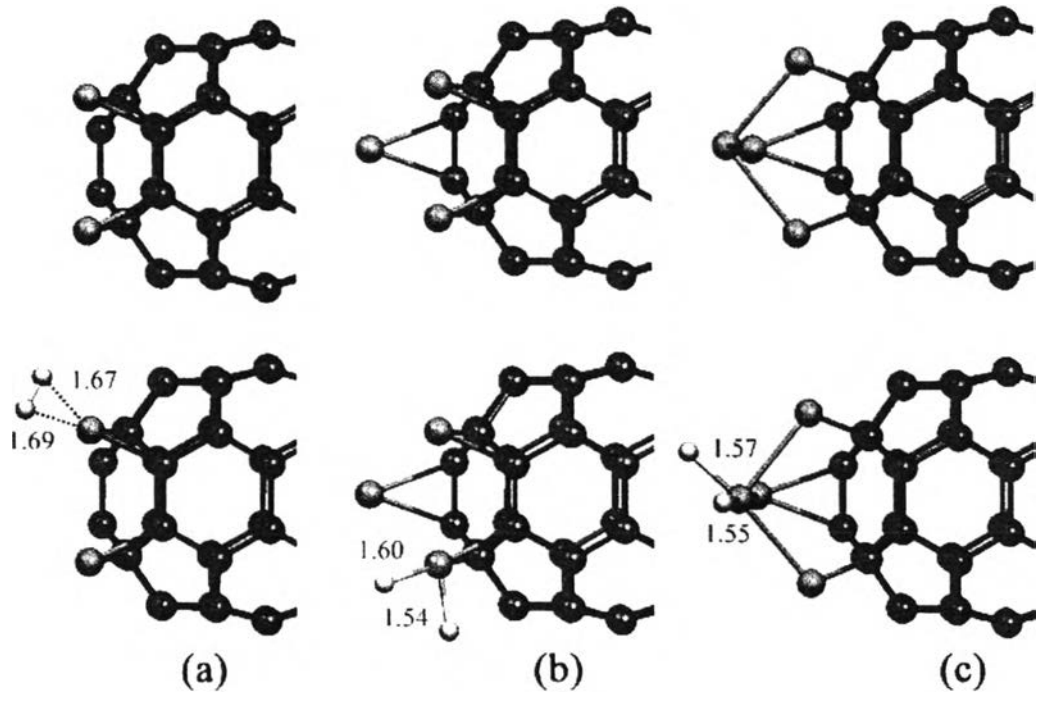

Figure 4.9 The B3LYP/GEN-optimized structures of adsorption configurations of H_2 adsorbed on Pt atom of the Pt cluster-decorated (4,4)SWCNTs whose Pt cluster are (a) Pt_2, (b) Pt_3 and (c) Pt_4. Top images are their bare Pt_n/SWCNTs structures. Their bond distances are in Å.

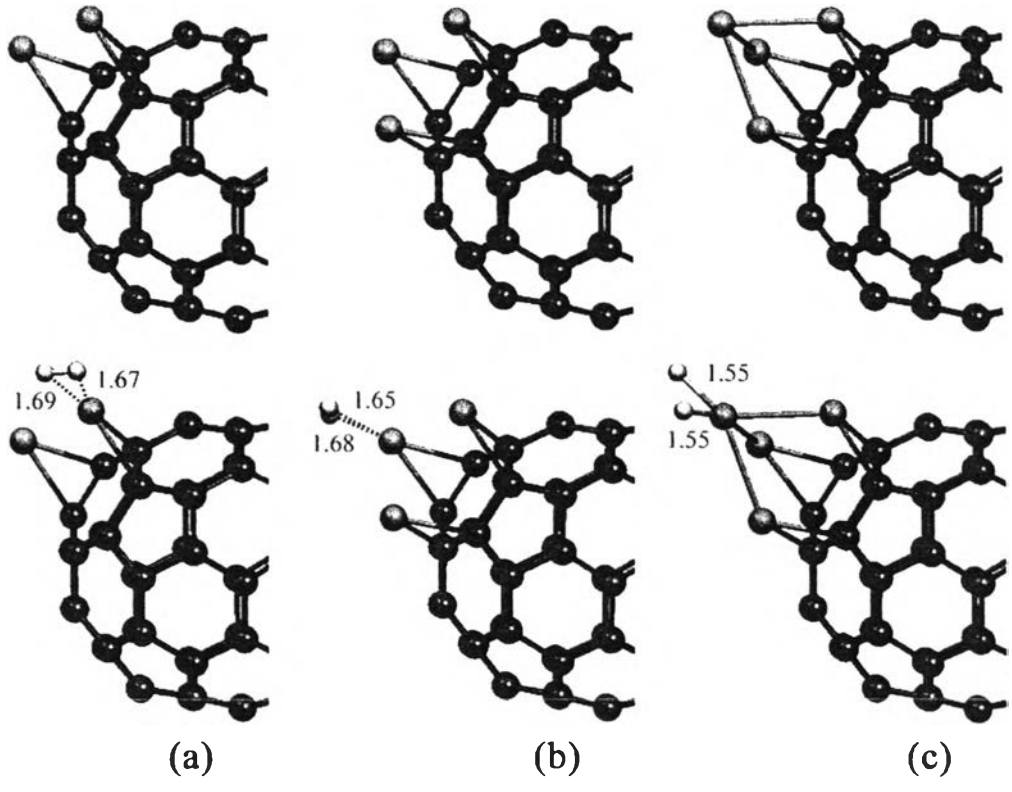

Figure 4.10 The B3LYP/GEN-optimized structures of adsorption configurations of H_2 adsorbed on Pt atom of the Pt cluster-decorated (5,5)SWCNTs whose Pt cluster are (a) Pt_2, (b) Pt_3 and (c) Pt_4. Top images are their bare Pt_n/SWCNTs structures. Their bond distances are in Å.

Table 4. 3 Binding energies of platinum clusters adsorbed on sidewall of various sizes of closed-end SWCNTs.

Pt clusters on SWCNTs	$\Delta E_{binding}$ [a]
On (3,3)SWCNT:	
Pt_2/(3,3)SWCNT	-63.90
Pt_3/(3,3)SWCNT	-67.68
Pt_4/(3,3)SWCNT[b]	-68.10
On (4,4)SWCNT:	
Pt_2/(4,4)SWCNT	-48.15
Pt_3/(4,4)SWCNT	-52.22
Pt_4/(4,4)SWCNT[b]	-60.55
On (5,5)SWCNT:	
Pt_2/(5,5)SWCNT	-31.04
Pt_3/(5,5)SWCNT	-41.52
Pt_4/(5,5)SWCNT[b]	-51.75

[a] In kcal/mol.

[b] Tetrahedral structure.

4.4 Hydrogen adsorption on platinum cluster decorated SWCNTs

Hydrogen adsorption configurations on platinum cluster decorated SWCNTs are shown in Figures 4.8, 4.9 and 4.10 for Pt_n/(3,3), Pt_n/(4,4) and Pt_n/(5,5)SWCNTs, respectively. It was found that adsorptions of hydrogen molecule on the Pt_2 of Pt_2/SWCNT and Pt_3 of Pt_3/SWCNT for all SWCNTs sizes are chemisorption but adsorptions of hydrogen molecule on Pt_4 (tetrahedral) of Pt_4/SWCNT for all SWCNTs sizes are dissociative chemisorption as shown in Table 4.4. The Pt_4 clusters of the most stable structures for Pt_4/(3,3), Pt_4/(4,4) and Pt_4/(5,5)SWCNTs are tetrahedral or distort tetrahedral structures and their hydrogen adsorption abilities correspond to the hydrogen adsorption on platinum atom of free platinum cluster Pt_4 (tetrahedral) (ΔE_{ads} = -26.03 kcal/mol) as shown in Figures A1, A2 and Table A2, in Appendix. Table A2 shows that hydrogen adsorption on the Pt_4 tetrahedral cluster is more

stable than on the Pt_4 square planar cluster (ΔE_{ads} = -20.54) by 5.49 kcal/mol. The dissociative chemisorption for hydrogen adsorption on Pt_4/SWCNTs were found and their abilities are in order: Pt_4/(3,3)SWCNT (ΔE_{ads} = -40.14 kcal/mol) > Pt_4/(5,5)SWCNT (ΔE_{ads} = -30.44 kcal/mol) > Pt_4/(4,4)SWCNT (ΔE_{ads} = -21.29 kcal/mol). The hydrogen adsorption on the Pt_4/(3,3)SWCNT is much stronger than on the Pt_2/(3,3)SWCNT and Pt_3/(3,3)SWCNT of which adsorption energies are -18.91 and -18.82 kcal/mol, respectively. But adsorption of hydrogen on the platinum cluster-decorated (4,4)SWCNT, the adsorption on the Pt_3/(4,4)SWCNT is the strongest and stronger than on the Pt_2/(4,4)SWCNT and Pt_4/(4,4)SWCNT. This may cause by size and shape effects of Pt clusters and (4,4)SWCNT. The hydrogen adsorption on the Pt_4/(5,5)SWCNT is a little stronger than on the Pt_2/(5,5)SWCNT and Pt_3/(5,5)SWCNT of which adsorption energies are -24.14 and -24.05 kcal/mol, respectively.

Selected geometrical parameters for free Pt_4 tetrahedral cluster and Pt_4 decorated on caps of (3,3), (4,4) and (5,5)SWCNTs are shown in Table A3. It shows that Pt_4 clusters on Pt_4/(3,3), Pt_4/(4,4) and Pt_4/(5,5)SWCNTs are distort tetrahedral structures of which Pt-Pt bonds of trigonal base are much longer than Pt-Pt bonds of free Pt_4 tetrahedral cluster. The B3LYP/LanL2DZ-optimized structures of free tetra platinum cluster (Pt_4) and Pt_4 decorated on caps of (3,3), (4,4) and (5,5)SWCNTs are shown in Figure A3.

Due to trigonal base of Pt_4 tetrahedral cluster interacting with three carbon atoms of (3,3), (4,4) and (5,5)SWCNTs caps over their hexagonal faces, hydrogen adsorptions on the Pt_4 tetrahedral cluster of Pt_4 decorated on caps of (3,3), (4,4) and (5,5)SWCNTs were therefore observed and compared to free tetra platinum cluster. Numbering for platinum atoms on free Pt_4 and Pt_4-decorated SWCNTs are labeled for using in comparison of their selected geometries. The adsorption energy diagram of hydrogen molecule on platinum atom of Pt_n decorated (3,3), (4,4) and (5,5)SWCNTs plotted against numbers (n) of platinum atom(s) of Pt_n clusters on SWCNTs are shown in Figure A4.

Table 4. 4 Hydrogen adsorptions on platinum atom of platinum clusters-decorated closed-end SWCNTs.

Hydrogen adsorption	ΔE_{ads} [a]
On Pt cluster/(3,3)SWCNT :	
H_2/Pt_2/(3,3)SWCNT[b]	-18.91
H_2/Pt_3/(3,3)SWCNT[b]	-18.82
H.H/Pt_4/(3,3)SWCNT[c]	-40.14
On Pt cluster/(4,4)SWCNT :	
H_2/Pt_2/(4,4)SWCNT[b]	-23.15
H_2/Pt_3/(4,4)SWCNT[b]	-31.24
H.H/Pt_4/(4,4)SWCNT[c]	-21.29
On Pt cluster/(5,5)SWCNT :	
H_2/Pt_2/(5,5)SWCNT[b]	-24.14
H_2/Pt_3/(5,5)SWCNT[b]	-24.05
H.H/Pt_4/(5,5)SWCNT[c]	-30.44

[a] In kcal/mol.

[b] Chemisorption.

[c] Dissociative chemisorption.

The zero-point vibration corrected energies (ZPE) and thermodynamic quantities for H_2 adsorbed to Pt on Pt_4 decorated SWCNTs were obtained and their equilibrium constants were derived from their free energy changes as shown in Table 4.5. All the hydrogen adsorptions are exothermic and spontaneous reactions 298 K. The preferred reactions for hydrogen adsorption processes on Pt atom of Pt-decorated SWCNTs are in order: the Pt_4/(3,3)SWCNT (ΔG_{298}= -23.99 kcal/mol) > Pt_4/(5,5)SWCNT (ΔG_{298}= -17.68 kcal/mol) > Pt_4/(4,4)SWCNT (ΔG_{298}= -3.02 kcal/mol). The equilibrium constant of hydrogen adsorption on the Pt_4/(3,3)SWCNT (K_{298}=

3.87×10^{17}) is very large and 2.40×10^{4} times larger than on the Pt_4/(5,5)SWCNT (K_{298} = 9.21×10^{12}) and 3.36×10^{15} times larger than on the Pt_4/(4,4)SWCNT (K_{298}= 9.21×10^{12}).

Table 4.5 Energetics, thermodynamic quantities and equilibrium constants of H_2 adsorbed to Pt on Pt_4 decorated armchair closed-end SWCNTs.

Reaction	$\Delta E^{a,b}$	$\Delta H_{298}{}^{b}$	$\Delta G_{298}{}^{b}$	K_{298}
H_2 + Pt_4/(3,3)SWCNT ⟶ H.H/Pt_4/(3,3)SWCNT	-39.36	-46.61	-23.99	3.87×10^{17}
H_2 + Pt_4/(4,4)SWCNT ⟶ H.H/Pt_4/(4,4)SWCNT	-19.82	-27.04	-3.02	1.64×10^{2}
H_2 + Pt_4/(5,5)SWCNT ⟶ H.H/Pt_4/(5,5)SWCNT	-29.59	-38.96	-17.68	9.21×10^{12}

[a] Zero-point vibration energy (ZPE).

[b] In kcal/mol.

4.5 Small gas adsorption on Pt_4 cluster- decorated SWCNTs

The optimized structures of adsorption configurations of CO, O_2, N_2, CO_2, N_2O, SO_2, H_2O, NO_2 and NH_3 on Pt_4/(3,3), Pt_4/(4,4) and Pt_4/(5,5)SWCNTs are shown in Figures 4.11, 4.12, 4.13, 4.14, 4.15, 4.16, 4.17, 4.18 and 4.19, respectively. Their adsorption energies are shown in Table 4.6. It was found that the adsorption of CO which are the highest strengths for Pt_4/(3,3) and Pt_4/(5,5)SWCNTs and their adsorption energies are -66.42 and -59.90 kcal/mol, respectively. For N_2O adsorption on the Pt_4/(4,4)SWCNT was found to be the strong adsorption (ΔE_{ads} = -49.17 kcal/mol).

Meanwhile, CO_2 adsorption showed the lowest adsorption abilities on Pt_4/SWCNTs for all SWCNTs sizes and their adsorption energies are -6.15, -1.23 and -7.19 kcal/mol for Pt_4/(3,3), Pt_4/(4,4) and Pt_4/(5,5)SWCNTs, respectively. The adsorption abilities of small gases are in orders: CO > NO_2 > O_2 > NH_3 > N_2 > SO_2 > N_2O > H_2O >> CO_2 for Pt_4/(3,3)SWCNT, NO_2 > CO > O_2 > NH_3 > SO_2 > H_2O > N_2 > N_2O >> CO_2 for Pt_4/(4,4)SWCNT and CO > O_2 > NO_2 > NH_3 > N_2 > H_2O > SO_2 > N_2O >> CO_2 for Pt_4/(5,5)SWCNTs.

Table 4.6 Adsorption energies of small gases on Pt_4 cluster decorated on various size close-ended SWCNTs.

Gas adsorption	ΔE_{ads} [a]		
	(3,3)SWCNT	(4,4)SWCNT	(5,5)SWCNT
Pt_4/SWCNT + CO → CO/Pt_4/SWCNT	-66.42	-44.54	-59.90
Pt_4/SWCNT + O_2 → O_2/Pt_4/SWCNT	-54.14	-42.12	-52.16
Pt_4/SWCNT + N_2 → N_2/Pt_4/SWCNT	-30.44	-12.42	-27.14
Pt_4/SWCNT + CO_2 → CO_2/Pt_4/SWCNT	-6.15	-1.23	-7.19
Pt_4/SWCNT + N_2O → N_2O/Pt_4/SWCNT	-23.70	-7.70	-21.76
Pt_4/SWCNT + SO_2 → SO_2/Pt_4/SWCNT	-24.72	-22.64	-23.53
Pt_4/SWCNT + H_2O → H_2O/Pt_4/SWCNT	-23.38	-17.97	-25.59
Pt_4/SWCNT + NO_2 → NO_2/Pt_4/SWCNT	-64.00	-49.17	-47.66
Pt_4/SWCNT + NH_3 → NH_3/Pt_4/SWCNT	-41.09	-31.07	-42.98

[a] in kcal/mol.

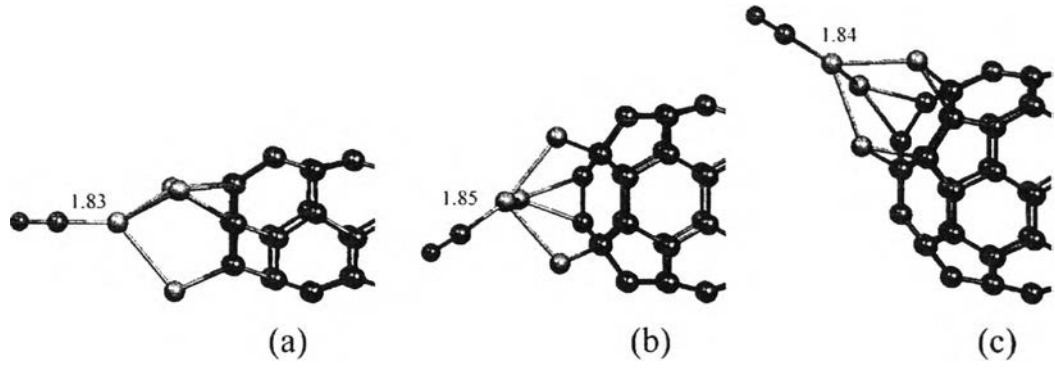

Figure 4.11 Adsorption configurations of CO adsorbed on Pt atom of the Pt_4 cluster-decorated closed-end as (a) (3,3), (b) (4,4) and (c) (5,5) armchair SWCNTs. Their bond distances are in Å.

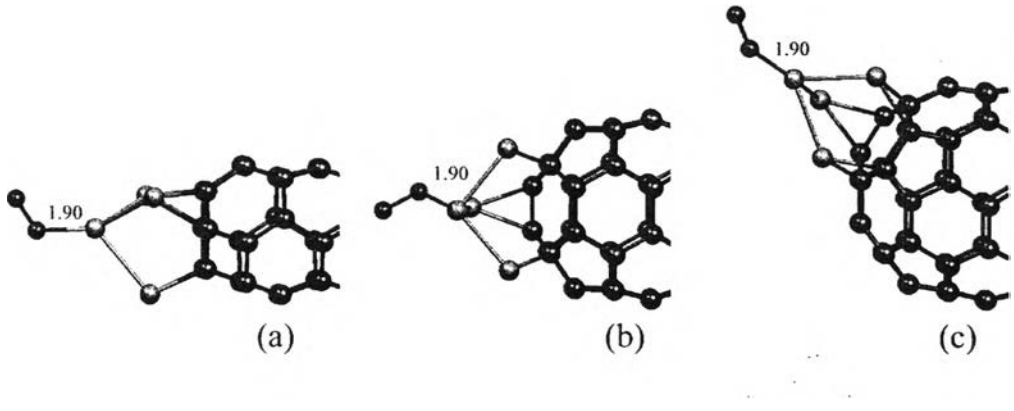

Figure 4.12 Adsorption configurations of O_2 adsorbed on Pt atom of the Pt_4 cluster-decorated closed-end as (a) (3,3) (b) (4,4) and (c) (5,5) armchair SWCNTs. Their bond distances are in Å.

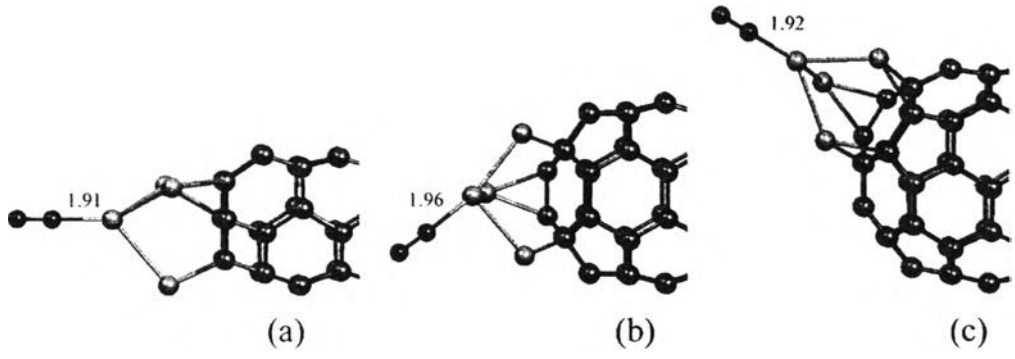

Figure 4.13 Adsorption configurations of N_2 adsorbed on Pt atom of the Pt_4 cluster-decorated closed-end as (a) (3,3), (b) (4,4) and (c) (5,5) armchair SWCNTs. Their bond distances are in Å.

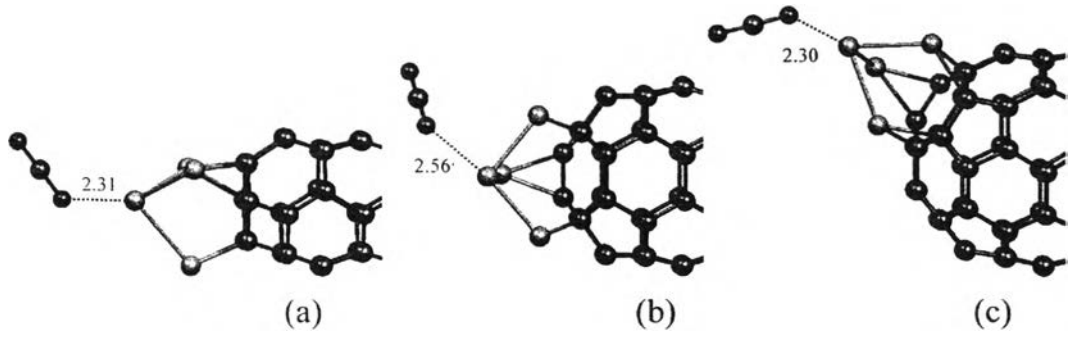

Figure 4.14 Adsorption configurations of CO_2 adsorbed on Pt atom of the Pt_4 cluster-decorated closed-end as (a) (3,3), (b) (4,4) and (c) (5,5) armchair SWCNTs. Their bond distances are in Å.

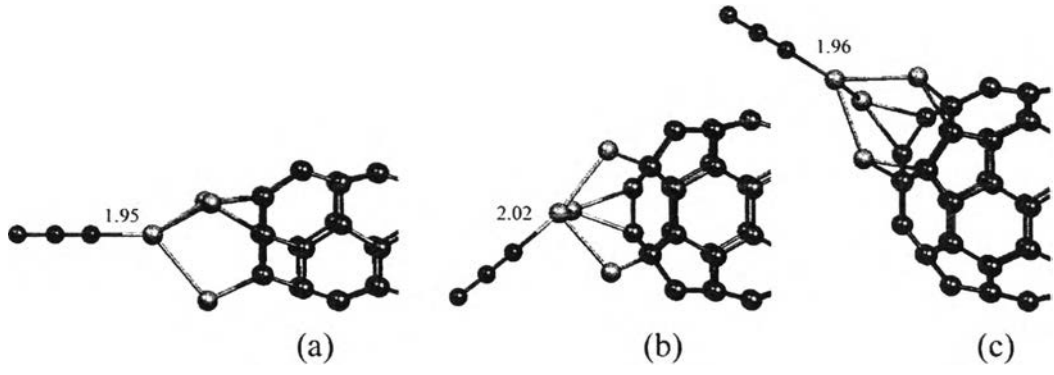

Figure 4.15 Adsorption configurations of N_2O adsorbed on Pt atom of the Pt_4 cluster-decorated closed-end as (a) (3,3), (b) (4,4) and (c) (5,5) armchair SWCNTs. Their bond distances are in Å.

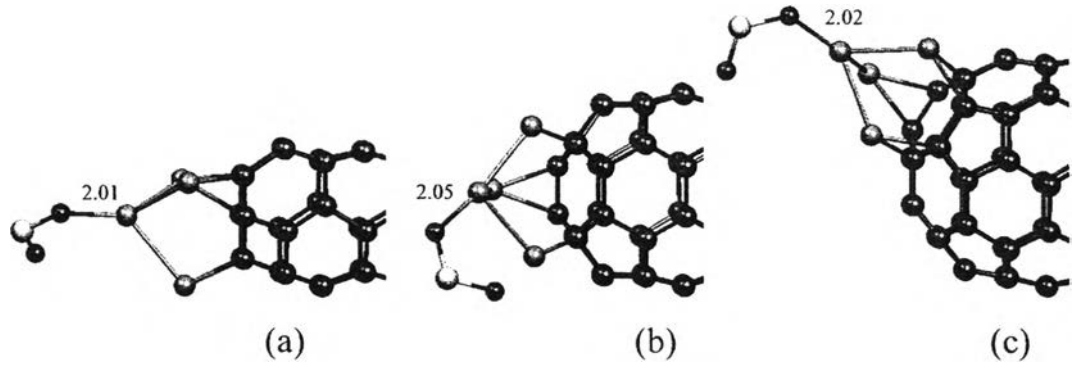

Figure 4.16 Adsorption configurations of SO_2 adsorbed on Pt atom of the Pt_4 cluster-decorated closed-end as (a) (3,3), (b) (4,4) and (c) (5,5) armchair SWCNTs. Their bond distances are in Å.

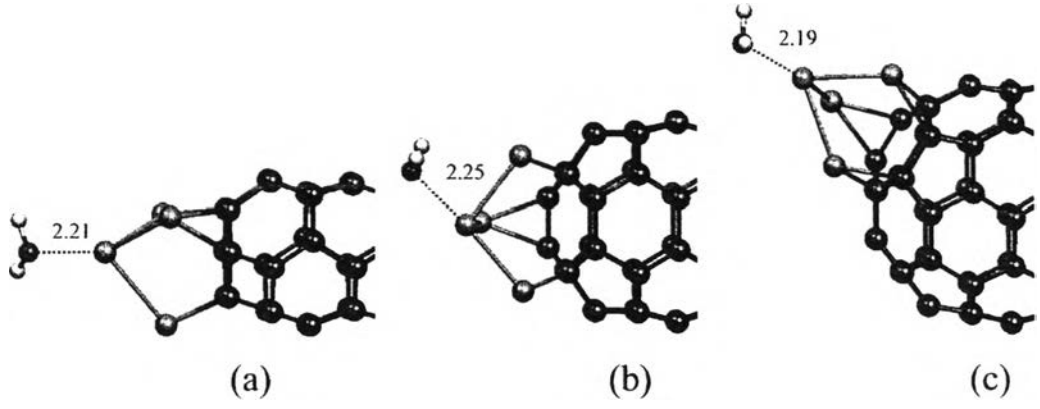

Figure 4.17 Adsorption configurations of H_2O adsorbed on Pt atom of the Pt_4 cluster-decorated closed-end as (a) (3,3), (b) (4,4) and (c) (5,5) armchair SWCNTs. Their bond distances are in Å.

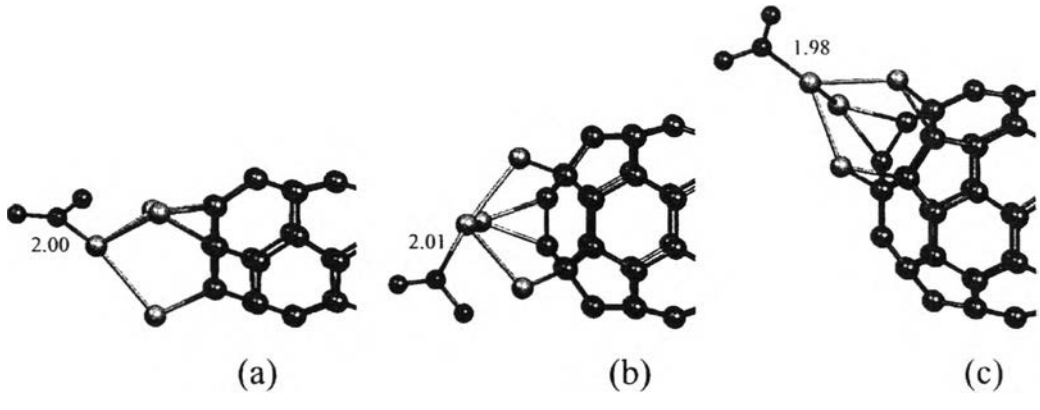

Figure 4.18 Adsorption configurations of NO_2 adsorbed on Pt atom of the Pt_4 cluster-decorated closed-end as (a) (3,3), (b) (4,4) and (c) (5,5) armchair SWCNTs. Their bond distances are in Å.

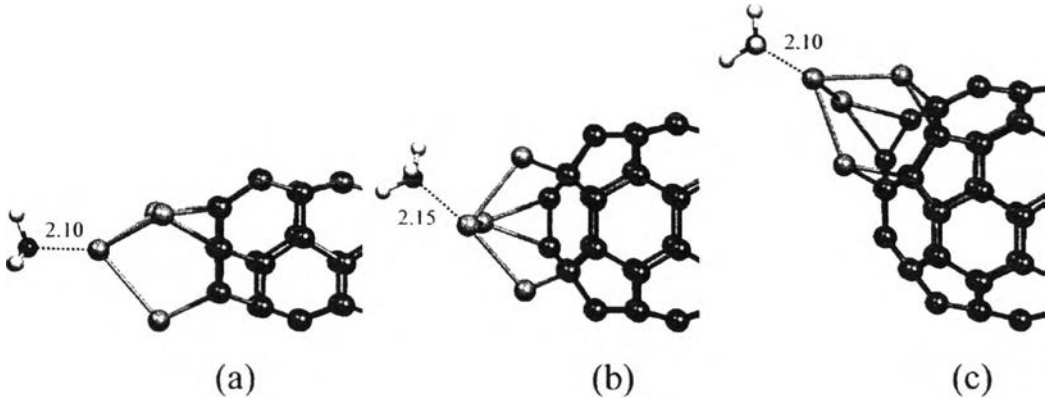

Figure 4.19 Adsorption configurations of NH_3 adsorbed on Pt atom of the Pt_4 cluster-decorated closed-end as (a) (3,3), (b) (4,4) and (c) (5,5) armchair SWCNTs. Their bond distances are in Å.

4.6 Binding of PGMs clusters on SWCNTs and their hydrogen adsorption.

The optimized structures of platinum group metal (PGM) as tetrameric clusters (Ru_4, Rh_4, Pd_4, Os_4, and Ir_4) on denoted C–C bonds at closed-end cap were obtained. It was found that all the tetrameric clusters of PGMs are distort tetrahedral structure. The geometrical parameters of PGMs-tetrameric clusters are shown in Figures 4.20, 4.21 and 4.22 for their binding structures on the (3,3)SWCNT, (4,4)SWCNT, (5,5)SWCNT, respectively.

The binding energies for PGMs adsorbed on sidewall of the various sizes of closed-end SWCNTs are listed in Table 4.7. The binding abilities of PGMs clusters on (3,3), (4,4) and (5,5)SWCNTs are in same order: Os > Ru > Ir > Rh > Pd. All various sizes of SWCNTs decorated by Os_4 are found that the interaction between Os_4 clusters and SWCNTs sidewall are the strongest as compared with others clusters.

The binding abilities of PGMs clusters on SWCNTs are in the same order: (3,3)SWCNT > (4,4)SWCNT > (5,5)SWCNT.

Table 4.7 Binding energies of PGMs clusters adsorbed on various sizes of close-ended SWCNTs.

Reaction	$\Delta E_{binding}$ [a]
PGMs clusters on SWCNTs:	
Ir_4 + (3,3)SWCNT ⟶ Ir_4/(3,3)SWCNT	-81.52
Ir_4 + (4,4)SWCNT ⟶ Ir_4/(4,4)SWCNT	-69.73
Ir_4 + (5,5)SWCNT ⟶ Ir_4/(5,5)SWCNT	-59.76
Os_4 + (3,3)SWCNT ⟶ Os_4/(3,3)SWCNT	-116.97
Os_4 + (4,4)SWCNT ⟶ Os_4/(4,4)SWCNT	-107.38
Os_4 + (5,5)SWCNT ⟶ Os_4/(5,5)SWCNT	-98.84
Pd_4 + (3,3)SWCNT ⟶ Pd_4/(3,3)SWCNT	-35.15
Pd_4 + (4,4)SWCNT ⟶ Pd_4/(4,4)SWCNT	-27.43
Pd_4 + (5,5)SWCNT ⟶ Pd_4/(5,5)SWCNT	-20.31
Rh_4 + (3,3)SWCNT ⟶ Rh_4/(3,3)SWCNT	-60.09
Rh_4 + (4,4)SWCNT ⟶ Rh_4/(4,4)SWCNT	-49.94
Rh_4 + (5,5)SWCNT ⟶ Rh_4/(5,5)SWCNT	-38.57
Ru_4 + (3,3)SWCNT ⟶ Ru_4/(3,3)SWCNT	-93.11
Ru_4 + (4,4)SWCNT ⟶ Ru_4/(4,4)SWCNT	-88.76
Ru_4 + (5,5)SWCNT ⟶ Ru_4/(5,5)SWCNT	-79.78

[a] in kcal/mol.

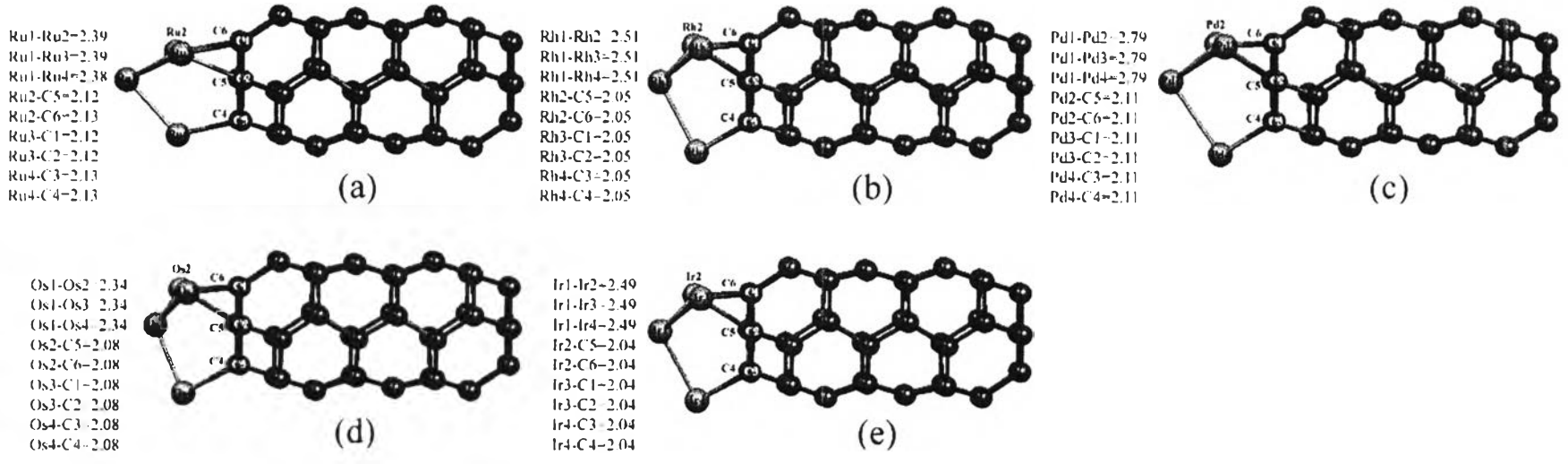

Figure 4.20 The B3LYP/GEN–optimized structures of closed–end (3,3) armchair SWCNT decorated (a) Ru_4, (b) Rh_4, (c) Pd_4, (d) Os_4, (e) Ir_4–doped SWCNTs.

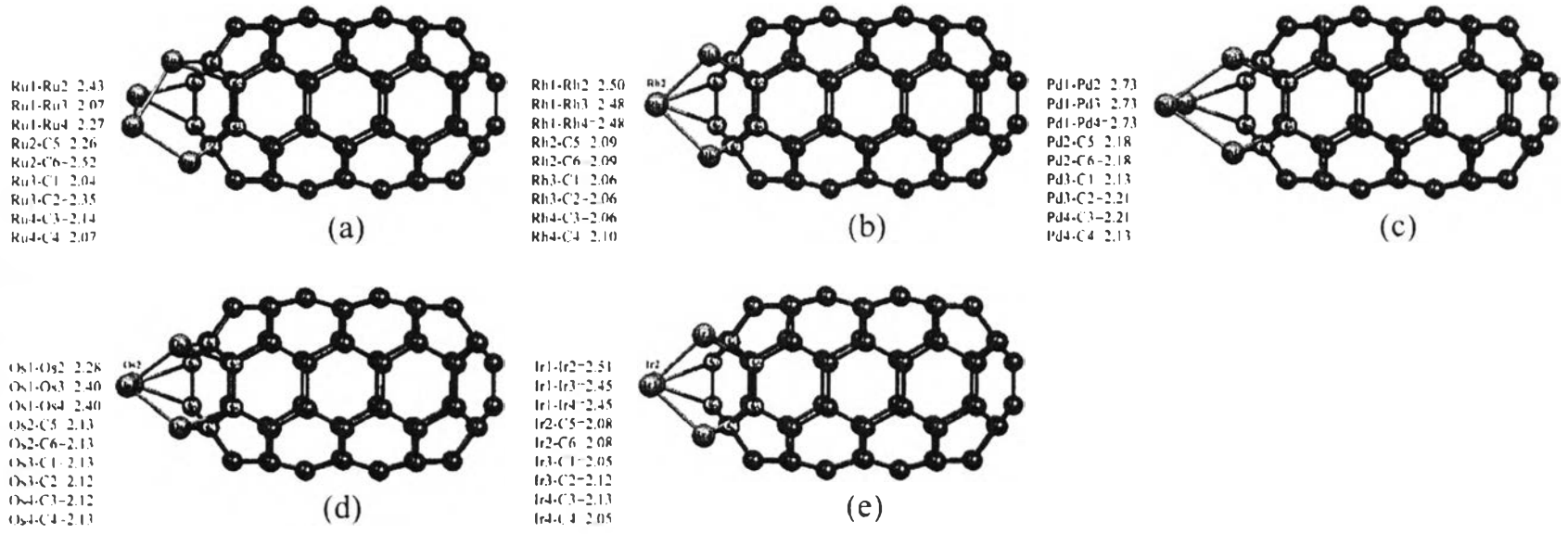

Figure 4.21 The B3LYP/GEN-optimized structures of closed-end (4,4) armchair SWCNT decorated (a) Ru_4, (b) Rh_4, (c) Pd_4, (d) Os_4, (e) Ir_4-doped SWCNTs.

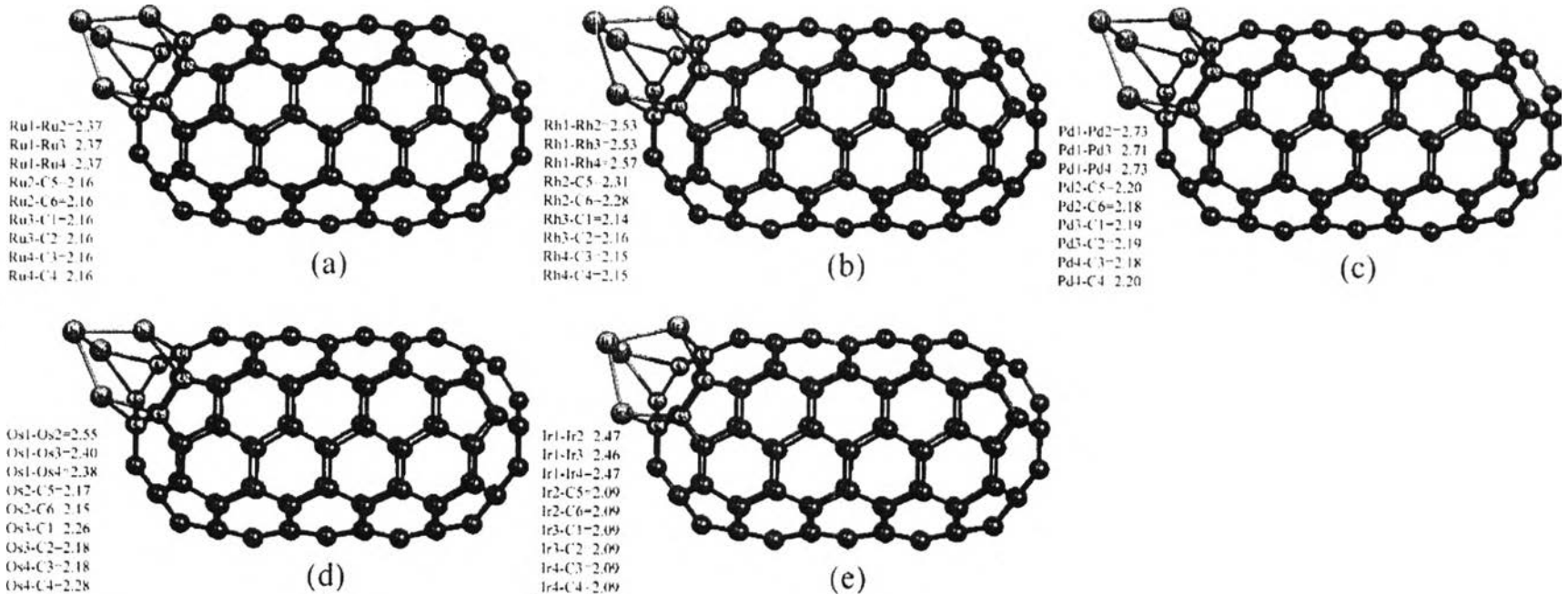

Figure 4.22 The B3LYP/GEN-optimized structures of closed-end (5,5) armchair SWCNT decorated (a) Ru_4, (b) Rh_4, (c) Pd_4, (d) Os_4, (e) Ir_4-doped SWCNTs.

Their hydrogen adsorption configurations are shown in Figures 4.23, 4.24 and 4.25 for PGM_n/(3,3), PGM_n/(4,4) and PGM_n/(5,5)SWCNTs, respectively. The hydrogen adsorption abilities on Ir_4, Os_4 and Rh_4/SWCNTs are in same order as (5,5) > (4,4) > (3,3)SWCNTs, but the abilities on Ru_4/SWCNTs is extremely different, which are in order: (4,4) > (3,3) > (5,5)SWCNTs. While, H_2 adsorbed on Pd_4/SWCNTs show slightly different on various sizes of SWCNTs.

It was found that adsorptions of hydrogen molecule on the Os_4 and Ir_4 of PGM_4/SWCNT for all SWCNTs sizes are dissociative chemisorption but adsorptions of hydrogen molecule on Pd_4, Ru_4, Rh_4 of PGM_4/SWCNT for all SWCNTs sizes are chemisorption as shown in Table 4.8. The dissociative chemisorption for hydrogen adsorption on Os_4/SWCNTs and Ir_4/SWCNTs were found and their abilities are in order: PGM_4/(3,3)SWCNT (ΔE_{ads} = −20.89, -18.11 kcal/mol) < PGM_4/(4,4)SWCNT (ΔE_{ads} = -42.76, -24.93 kcal/mol) < PGM_4/(5,5)SWCNT (ΔE_{ads} = −43.13, -24.95 kcal/mol).

The hydrogen adsorption on the Os_4/(5,5)SWCNT and Ir_4/(5,5)SWCNT are slightly different as compared with the Os_4/(4,4)SWCNT and Ir_4/(4,4)SWCNT, respectively. The hydrogen adsorption on the Os_4/SWCNT is much stronger than on the Ir_4/SWCNT.

Table 4.8 Adsorption energies of H_2 on metals cluster of various sizes close-ended SWCNTs.

Hydrogen adsorption	ΔE_{ads} [a]
PGMs clusters on SWCNTs :	
H_2/Ir_4/(3,3)SWCNT[b]	-18.11
H_2/Ir_4/(4,4)SWCNT[b]	-24.93
H_2/Ir_4/(5,5)SWCNT[b]	-24.95
H_2/Os_4/(3,3)SWCNT[b]	-20.89
H_2/Os_4/(4,4)SWCNT[b]	-42.76
H_2/Os_4/(5,5)SWCNT[b]	-43.13
H_2/Pd_4/(3,3)SWCNT	-16.08
H_2/Pd_4/(4,4)SWCNT	-16.91
H_2/Pd_4/(5,5)SWCNT	-16.80
H_2/Rh_4/(3,3)SWCNT	-8.19
H_2/Rh_4/(4,4)SWCNT	-10.42
H_2/Rh_4/(5,5)SWCNT	-20.73
H_2/Ru_4/(3,3)SWCNT	-9.02
H_2/Ru_4/(4,4)SWCNT	-14.21
H_2/Ru_4/(5,5)SWCNT	-8.36

[a] in kcal/mol.

[b] Dissociative adsorption.

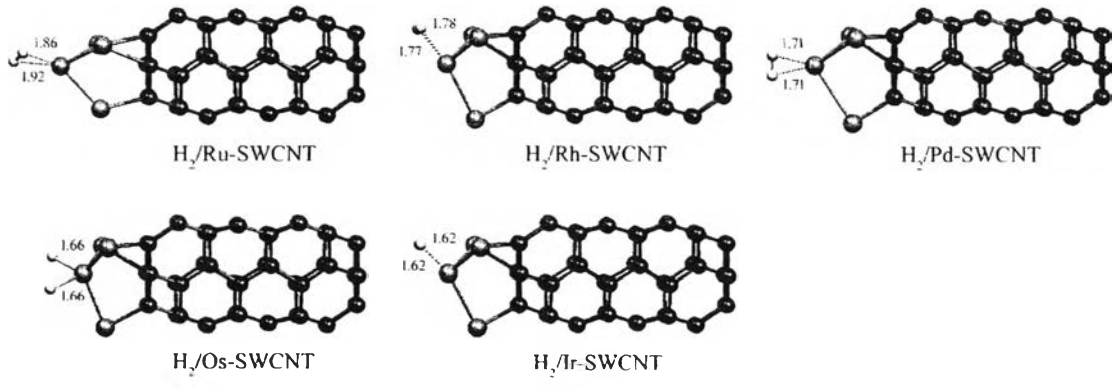

Figure 4.23 The B3LYP/GEN-optimized structures of adsorption configurations of H_2 adsorbed on metal atom of (a) Ru_4, (b) Rh_4, (c) Pd_4, (d) Os_4, (e) Ir_4-doped of closed-end (3,3)SWCNTs.

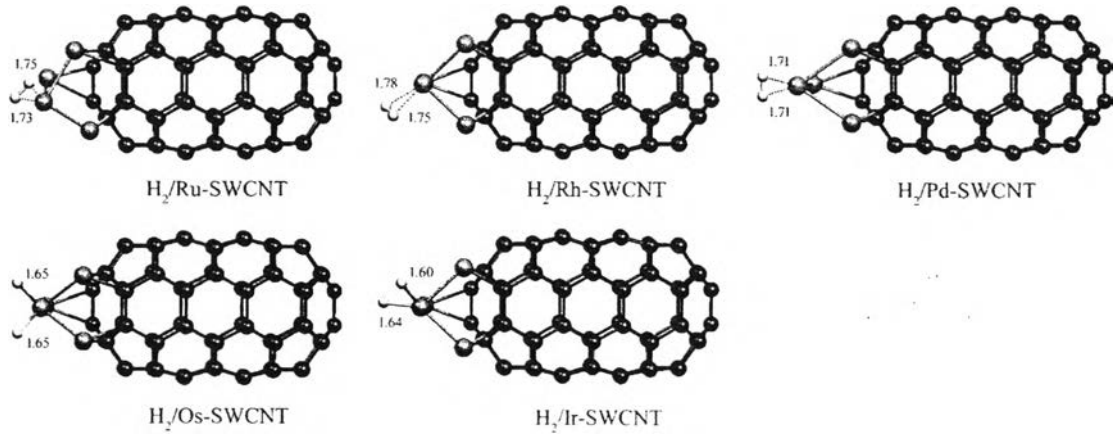

Figure 4.24 The B3LYP/GEN-optimized structures of adsorption configurations of H_2 adsorbed on metal atom of (a) Ru_4, (b) Rh_4, (c) Pd_4, (d) Os_4, (e) Ir_4-doped of closed-end (4,4)SWCNTs.

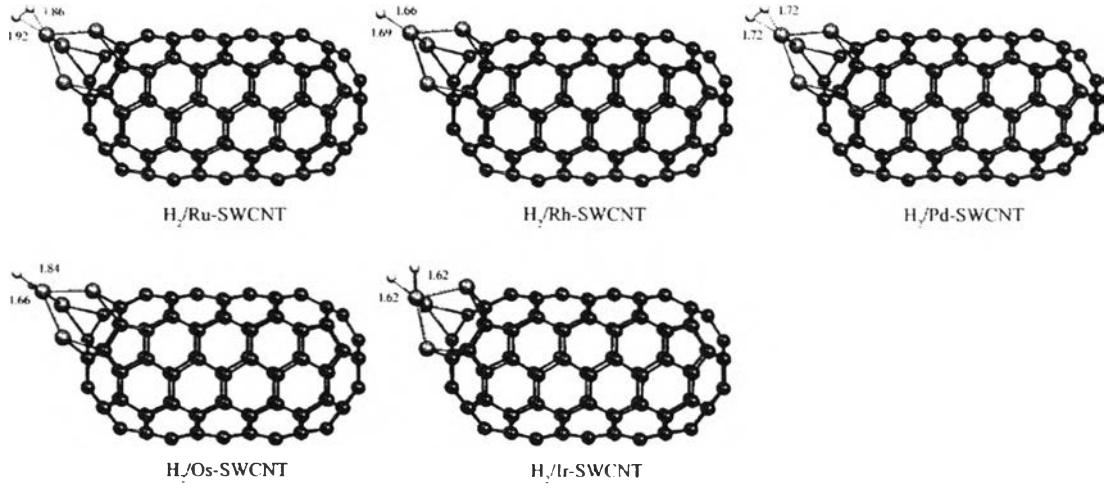

Figure 4.25 The B3LYP/GEN-optimized structures of adsorption configurations of H_2 adsorbed on metal atom of (a) Ru_4, (b) Rh_4, (c) Pd_4, (d) Os_4, (e) Ir_4-doped of closed-end (5,5)SWCNTs.